A Comparative Deep Learning Framework for Automated Lung Cancer Detection and Classification Using CNN and Residual Networks.

Abstract:

Lung cancer is one of the major causes of death that arise from various kinds of cancers. For this reason, early diagnosis and classification of the disease is essential for treatment purposes. A model for the detection and classification of lung cancer was developed in this study using CT scans of lungs. This involved the use of the CNN and ResNet50 algorithms to detect and classify features in the model. Various image pre-processing methods, such as resizing, normalizing, filtering, and augmenting the images were performed before the process of classification began using the binary and multiclass methods.

The accuracy achieved in the experiment was fairly accurate in the classification of lung cancer. Accuracy of about 98.08% was attained using the two methods. However, higher accuracy was recorded using the ResNet50 algorithm than using the CNN algorithm for multiclass classification. Accuracy attained was 97.10% and 96.54%, respectively.

Keywords:-

Lung Cancer Detection, Deep Learning, Convolutional Neural Network (CNN), ResNet50, CT Scan Images, Medical Image Classification, Binary Classification, Multiclass Classification, Feature Extraction, Artificial Intelligence in Healthcare.

Introduction:-

Lung cancer is the uncontrolled growth of abnormal cells in the lungs, and is one of the major causes of cancer-related deaths worldwide. The early detection is a crucial factor in achieving a better outcome and prompt intervention of more effective and less invasive treatments. Lung cancer leads to almost 1.8 million deaths annually, making it the leading cause of cancer-related mortality worldwide, according to the World Health Organization (WHO). Recent improvements in early diagnosis and treatment techniques have helped to slowly decrease death rates. There are some risk factors that increase the risk of lung cancer; smoking is the most important and is responsible for almost 90% of lung cancer cases. Other factors involve lifestyle, drinking excessive amounts of alcohol, air pollution, genetic makeup and exposure to toxic substances.

Chest pain, difficulty breathing, tiredness, coughing up blood or having blood in the urine, constant cough, wheezing, and weight loss are some symptoms of lung cancer. Lung cancer is generally classified into two categories: Small cell lung carcinoma and non-small cell lung carcinoma, with adenocarcinoma or squamous cell carcinoma being the common types of non-small cell lung carcinoma. Diagnosing lung cancer involves a physical examination, imaging tests (X-ray, computed tomography (CT) and magnetic resonance imaging (MRI) scans) and biopsy testing (which involves studying a sample of tissue). The treatment will depend on the type and stage of the cancer and may include surgery, chemotherapy, radiation, targeted therapy and immunotherapy.

In recent years, medical imaging has been a crucial part of the detection and classification of lung cancer, and machine learning and deep learning technologies have been becoming more prominent. In recent years, algorithms such as Support Vector Machine (SVM), K-Nearest Neighbor (KNN), Random Forest, Logistic Regression, Gradient Boosting, AdaBoost and deep neural networks have been gaining popularity to improve diagnostic accuracy and to facilitate the early detection of the disease.

RELATED WORK:-

Machine learning and deep learning have been used in several studies for the diagnosis of lung cancer. Many attempts have been made to analyze the medical imaging data set of TCIA, TCGA, LIDC-IDRI, LUNA16 and achieved High accuracy using Deep Learning and Machine Learning models. Sangeetha et al. [1] have presented a Multimodal Fusion Deep Neural Network (MFDNN) using preprocessing and augmentation, which achieved an accuracy of 92.5%. Hybrid models, such as 3D CNN and RNN models were also designed for early lung

cancer detection and classification. The accuracy achieved by Noseer et al. [4] is 97.98% on the LUNA16 dataset using a modified AlexNet-SVM approach, while Shah et al. [5] used deep 2D CNN classifier with 95% accuracy.

Other studies used state-of-the-art preprocessing techniques and hybrid learning methods. To enhance accuracy in classification, Davri et al. [6] applied techniques like GANs, semi-supervised learning, and stacked autoencoders. Srivastava et al. [7] used a Hybrid Faster R-CNN model on MRI and CT to achieve a detection accuracy greater than 97%. Mohamed et al. [8] used image preprocessing techniques and CNN along with metaheuristic algorithms to achieve 93.21% accuracy. Maleki et al. [9] fused traditional machine learning models SVM, Random Forest and Gradient Boosting with CNN and ANN models with 95% accuracy. Other researches with the help of the X-ray and CT, also showed the efficacy of CNN-based and deep-learning techniques in the diagnosis of lung cancer.

Furthermore, when using chest X-ray and CT images for multi-classification, a deep learning model proposed by Ibrahim et.al [12] with VGG19-CNN architecture attained 98.05% accuracy with high precision, recall and specificity. Chaunzwa et.al [13] used convolutional neural networks (CNNs) as the main classifier to predict the tumor histology. Furthermore, CNN-based quantitative radiomics features were used in machine learning classifiers such as k-nearest neighbors (KNN) and support vector machine (SVM). The CNNs were shown to be capable of the prediction of the histology of the tumor with an AUC of 0.71 ($p = 0.018$), while Zhao et.al [14] suggested using a weighted discriminative approach and an Artificial Learning Machine for detecting lung cancer by using an electronic nasal device. Using targeted metabolomic analysis via LC-MS/MS, Xie et.al [15] evaluated 61 plasma metabolites and applied 6 machine learning techniques to the development of an early prediction model of lung tumor by selecting the above-mentioned metabolites, with their respective performances ranging from 89.5% to 97.4% accuracy on the test set and 89.6% to 97.4% accuracy on the training set. In the ACDC@LungHP challenge, Zhang et.al [16] used a pre-processing step of noise filtering, followed by the Otsu algorithm to eliminate the background area in the tumor tissue labels, and used a dataset of 150 images for training and 50 images for testing with a total of 200 patients to obtain a more accurate boundary of the cancer area by deep learning. In this CT images, Yu et.al [17] is used and the pre-processing enhances the quality of the images obtained from the CT scanner by adjusting pixel intensities and eliminating inconsistent and noisy pixels.

This segmentation contains a K-mean algorithm to segment the region affected by cancer in CT images. It uses a Deep Neural Network for the detection of lung cancer and an Adaptive Hierarchical Heuristic Mathematical Model for which it has an accuracy of 96.67% for the absence or presence of lung cancer. In this work, Masood et.al [18] uses CT images and their image data preprocessing consists of rescaling the image and data augmentation with transformation such as translation, scaling and rotation to minimize overfitting. It involves the use of improved MRFCN (which is a multidimensional Region-based Fully Convolutional Network) with an accuracy of 97.91% as a classifier. The dataset [19] used in the study contains 939 digitalized histology WSIs of 871 lung cancer patients and 68 healthy subjects and annotations for various lung cancer classes. The preprocessing methods include downscaling each WSI by 4 to 1 mm pixel and applying data augmentation techniques like rotation, translation, flipping, and color jittering to augment the training set. It adopts an RF classifier to make the prediction of WSI level and the accuracy can reach 97.3% in lung cancer image classification. Shakeel et.al [20], the lung CT images for this study were collected from the Cancer Imaging Archive (CIA) dataset.

Weighted mean histogram equalization was employed to remove noisy data and profuse clustering technique was improved to enhance lung images. This study adopted the Deep Learning Instantaneously Trained Neural Network (DITNN), which is a classifier for predicting lung cancer. The accuracy rate of the system was 98.42% with the lowest classification error being 0.038. The LIDC-IDRI database included clinical chest computed tomography (CT) scans which were preprocessed by Xie et.al [21] who segmented the nodules slice-by-slice with a trained U-Net network. Multi-view Knowledge-based collaborative deep model was used as a classifier in the MV-KBC method and its accuracy was 91.60%. Lakshmana Prabu et.al [22] have classified the CT lung images with the support of supervised machine learning techniques, as presented in this.

The preprocessing involves image quality improvement and feature extraction such as histogram, texture, and wavelet analysis. The classifier is a deep neural network (DNN) which is trained by the Modified Gravitational Search Algorithm (MGSA). The proposed classifier gives the sensitivity value of 95.26%, specificity value of 96.2% and overall accuracy value of 96.2%. The dataset is CT images of lung cancer, the pre-processing is noise removal, histogram equalization and data augmentation as provided by Pang et.al [23]. The classification system consisted of a densely connected convolutional network (DenseNet), which was used to classify malignant tumors based on computed tomography (CT) images, with adaptive boosting algorithm (AdaBoost)

being used for aggregation of classification results. The method was able to obtain an identifying accuracy of 89.85%, which is higher than other models such as ResNet, VGG16, and AlexNet.

The literature survey on the current research work done on the identification of lung cancer with deep learning algorithms suggests that the future looks promising with great expectations of advancements and further research. The success of deep learning architectures for medical image-based lung cancer detection has been demonstrated in numerous research studies, such as computed tomography (CT) scans and X-rays. It has the potential to transform the early detection and diagnosis of such models by combining and outdoing conventional approaches. Moreover, the survey presents the variety of methodologies used, such as convolutional neural networks (CNNs) and recurrent neural networks (RNNs). Each of these methods presents their advantages and disadvantages regarding the accuracy, speed and comprehension in the research and healthcare arenas.

PROPOSEDMETHOD:-

The manuscript introduces a theoretical framework tailored to forecast occurrences of lung carcinoma. The framework commences by processing the data, subsequently proceeding with feature extraction and classification through the employment of a sophisticated deep learning technique referred to as Convolutional Neural Network (CNN). A visual representation of the outlined approach is illustrated in Figure 1:

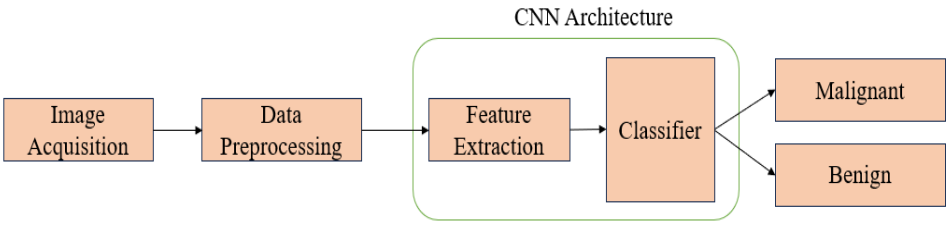

Fig 1. Shows the basic block diagram

Image Acquisition:-

CT images of lung cancer from Kaggle datasets are a set of medical images obtained by a computed tomography (CT) scanner, especially lung tissue. These datasets are usually curated for research purposes and provideresearchers and developers access to a large volume of anonymized patient data for a range of computational tasks such as image analysis, computer aided diagnosis and machine learning algorithm development.

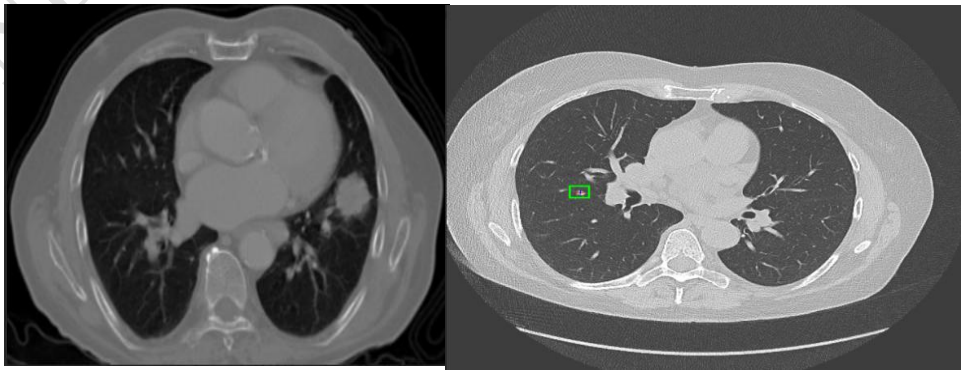

(a) (b)

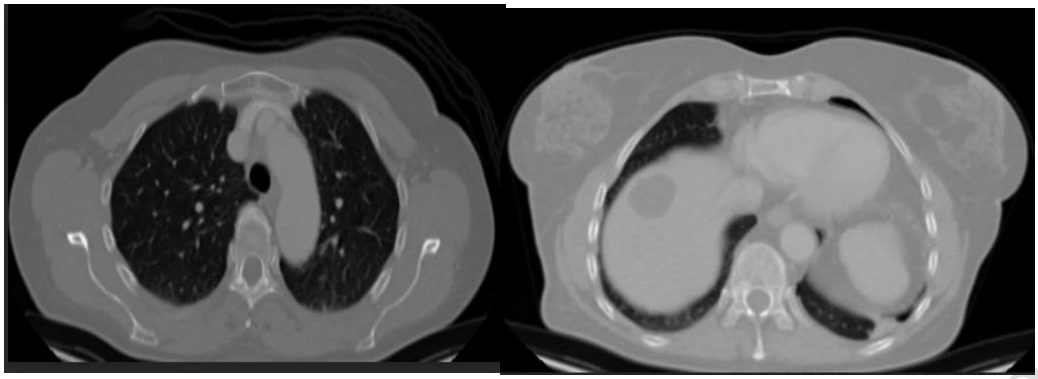

(c) (d)

Fig 2. Various CT images. (a) Squamous cell carcinoma (b) Normal (c) Large cell carcinoma (d) Adenocarcinoma

The CT images in these datasets are cross-sectional slices of the patient's chest, which allow for detailed visualization of the lung anatomy. These are usually high resolutiongray scale images in which the intensity of each pixel depends on the density of the tissue in the lung. These CT images are then used by researchers to study the features and presentation of lung cancer. They may also contain annotations of the images indicating regions of interest (e.g. nodules, masses or other abnormalities) to facilitate development and evaluation of automated detection and classification algorithms.

Data Preprocessing:-

In a CNN (Convolutional Neural Network), data preprocessing for CT images includes dataset splitting, normalization and image resizing. Image resizing is a cost-effective process without losing significant features. Normalization is a technique for standardizing the pixel values typically in the range of 0 to 1, to enhance training performance and convergence. The dataset is then split into training, validation and testing sets, to train the model, fine-tune the parameters, and test it. The proposed preprocessing methods enable the CNN model to effectively capture the significant features and patterns in the CT images.

Feature extraction and Classification:-

For this research, Deep Learning techniques have been employed with the use of CNN as a means of extracting features and doing classification. In addition to that, the ResNet model was utilized in this study. The Convolution Neural Network (CNN) is an evolution of the Artificial Neural Network (ANN), which is mostly used to extract features from grid-like matrix data structures. The CNN simplifies image and video processing as it is a Deep Learning neural network. Features within images and videos are first extracted through CNN using convolutions and pooling, and then the network detects/classifies the object/scene on the basis of those features.

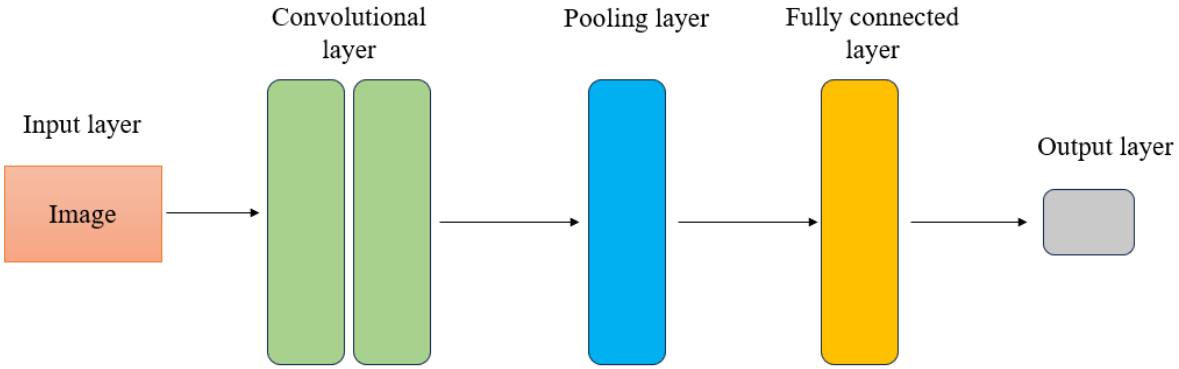

Fig 3. Architecture of CNN

The convolution layer extracts features by using filters, the pooling layer reduces the computational complexity, and the fully connected layer makes a prediction based on these features. In order to process an image or a video, CNNs use multiple layers of convolutional and pooling operations. A small-sized filter, or a kernel, is slid over the input image/video to extract features by calculating the dot product of the filter and the input. These layers' output is down sampled in order to reduce the dimensionality of the data.

A comprehensive architecture of Convolutional Neural Networks is commonly referred to as covnet. Covnets consist of a sequence of layers, with each layer performing a differentiable function that transforms one volume into another. Various types of layers are:

Input Layers: They are used to provide input to the model either in the form of an image or sequence of images depending on whether we are working with CNN.

Convolutional Layer: This is used to get features from the input using what is called learnable kernels which go through the image and calculate the dot product between them. The shape of these kernels is mostly either 2x2, 3x3, or 5x5.

Activation Function: Non-linearity is added to the network via an element-wise function that operates on the output of the previous layer. The activation functions include RELU, Tanh, and Leaky RELU among others, where we are using RELU.

Pooling Layer: A common component in convnets, the pooling layer reduces the volume size to improve computational efficiency, minimize memory requirements, and mitigate the risk of overfitting. The two commonly applied pooling techniques are max pooling and average pooling, where max pooling has been adopted in this instance.

Fully Connected Layers: This takes input from the previous layer and processes the input for making the final classification or regression operation. The output of the fully connected layers is finally sent to logistic functions such as sigmoid and SoftMax for classifications, thereby converting the output to probabilities associated with each class.Overall, CNNs demonstrate tremendous success in dealing with the problem of classifications, detections, and segmentation owing to their ability to automatically extract information hierarchies.

ResNet

ResNet, known as Residual Networks, is an example of complicated neural networks designed to deal with the problem of the vanishing gradient effect seen in very deep neural networks. Vanishing gradient effect arises during training, where gradients become negligible, thereby creating hurdles for the network to learn. The major innovation in ResNet is its use of residual connections that help the network learn residual mappings instead of the actual mappings. Residual connections make sure that the gradients flow more efficiently in complex networks, thereby helping to train very deep neural networks in comparison to normal architectures.

The working of ResNet is because of the use of the following components:

Basic Block: Some of the basic components used in ResNet include the use of residual block that uses two convolutional layers connected by the shortcut connection. The shortcut connection makes it possible to skip some of the convolutional layers, adding the input to the output of the residual block in order to make residual mapping.

Adding Identity Mapping: The use of shortcut connection during the formation of the residual mapping makes it possible to ensure that there is no loss experienced on the output resulting from the residual block in terms of initial input. When the initial features are sufficient to perform the task, it becomes possible to disable the residual block by making convolutional layers zero.

Stacking of Blocks Method: The ResNet architecture is made up of stacking many residual blocks. With more residual blocks used, more complicated architectures are developed, which allow for deeper architectures.

Down sampling Technique: Besides using residual blocks, the ResNet models also employ down sampling techniques that involve the use of max pooling layers or convolutional layers where the stride value exceeds 1.

ResNet50 was used in the research to detect lung cancer. This is a deep learning technique that has a total of fifty layers and is well-known because of the accuracy that it achieves compared to other neural network

techniques and their ability to perform computationally. ResNet50 helps to classify the images in terms of cancer cells and healthy cells by learning more about them using its residual connections.

RESULT AND DISCUSSION:-

Detection of Lung Cancer by Using Deep Learning is based on the analysis of the images from CT scans using deep learning neural networks to detect cancer areas in the lung scans. Image preprocessing methods such as normalization, resizing, and data augmentation have been carried out to optimize the performance of the model and to increase its speed of processing. Popular Deep Learning models are Convolutional Neural Networks and ResNet50, which are employed for classification purposes. In our experiment, we conducted both binary and multiclass classifications of images as follows.

BINARY CLASSIFICATION:-

When it comes to binary classification, the models were designed for distinguishing between adenocarcinoma and normal tissue on CT scans. Adenocarcinoma can be regarded as one of the most widespread types of non-small cell lung cancer, while normal tissue implies healthy lungs without any signs of cancer. Such machine learning approaches as CNN and ResNet50 were used for this purpose.

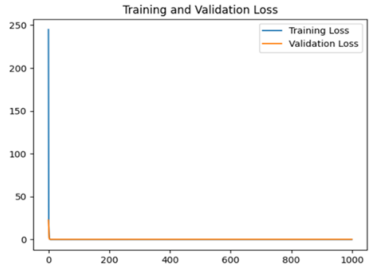

Figure 2 displays the loss during training and validation of the Convolutional Neural Networks model through 1000 epochs. The losses during both training and validation tend to drop to zero continuously, which means the model has learned well and generalized well.

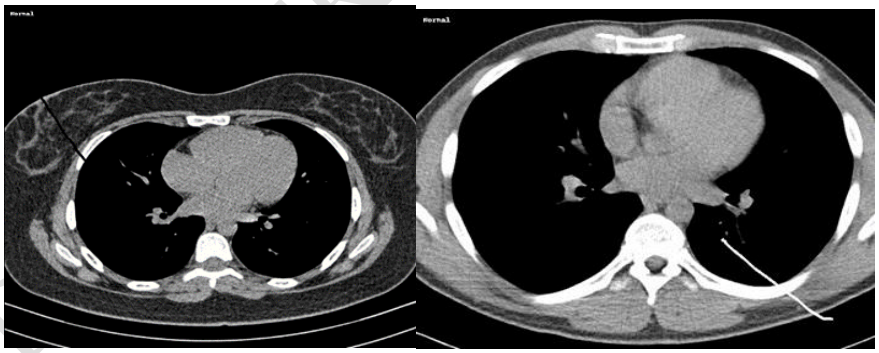

(a) (b)

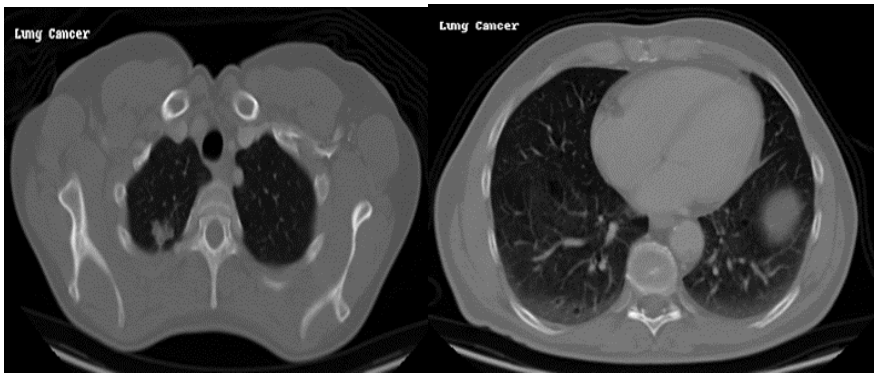

(c) (d)

Fig Results of Binary Classification with CNN (a) (b) Normal, (c) (d) Lung Cancer

The chart below represents the results of the binary classification performed by a model of Convolutional Neural Networks for images captured from CT scans. The images (a) and (b) belong to the category of healthy lungs, whereas images (c) and (d) have been classified as lung cancer cases.

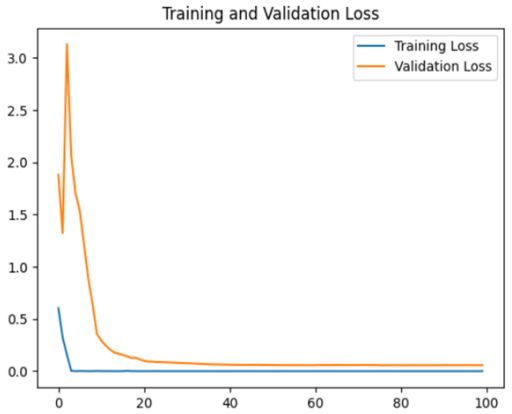

In the diagram below, you can observe how the training and validation losses of the ResNet50 model vary across several epochs. The significant drop in the loss levels shows that the model has learned crucial features from the training set well enough. Moreover, the training and validation loss curves converge, which means there is no significant overfitting and, hence, the model works well on unseen samples.

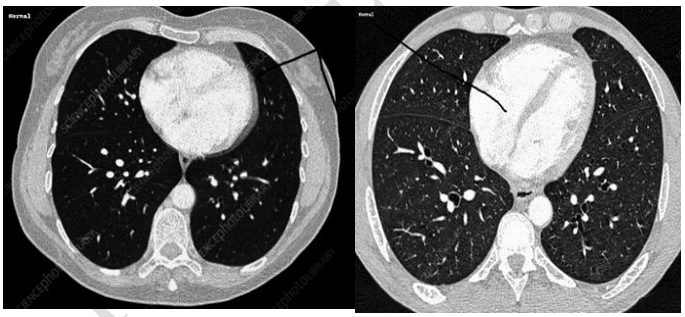

(a) (b)

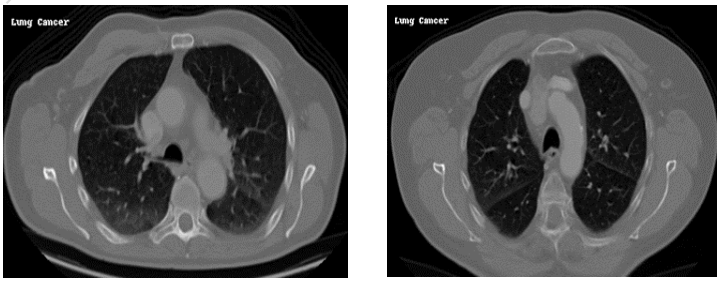

(c) (d)

Fig Results of Binary Classification using ResNet (a) (b) normal (c) (d) Lung Cancer

The figure illustrates the results of a binary classification exercise that was carried out using ResNet to classify normal and lung cancer cases from medical images. The figure successfully demonstrates the capability of the ResNet model in classifying normal and lung

cancer cases from medical images. Examples of normal and cancer cases have been included to emphasize the difference in the images used.

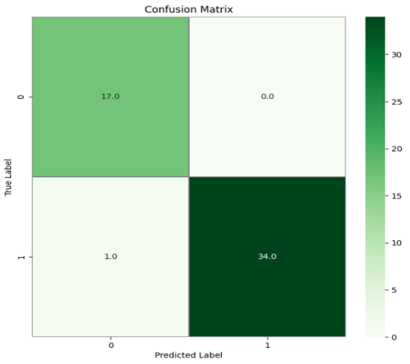

Fig Confusion Matrix of Binary Classification with CNN

The confusion matrix of the CNN model utilized for the classification of binary cancer instances is provided in the figure given below in Figure 4.1.e. The CNN model categorizes the CT scans of the lungs in class 0, where there is no presence of cancer, or class 1, indicating the presence of cancer. The confusion matrix evaluates the performance of the classifier in terms of metrics such as True Positive (TP), True Negative (TN), False Positive (FP), and False Negative (FN). The confusion matrix suggests 17 true negatives, 34 true positives, 0 false positives, and 1 false negative. The greater the color intensity, the larger the number of correctly classified instances.

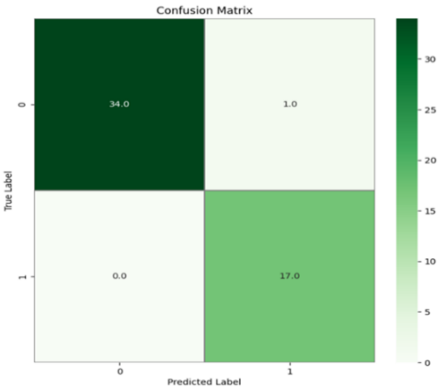

Fig Confusion Matrix of Binary classification with ResNet

The confusion matrix of the model ResNet50 which was used to classify the cases into two classes for lung cancer is depicted in Figure 4.1.f below. The ResNet50 model identified 34 true negatives and 17 true positives. One false positive case was predicted by the model without any false negatives being predicted. This implies that the model is efficient in the classification process. The confusion matrix highlights that the model is able to accurately distinguish between the cancerous and non-cancerous cases.

Accuracy: Accuracy is the ratio of correctly predicted instances to the total instances.

$$Accuracy = \frac{TP+TN}{TP+FN+FP+TN} \qquad (1)$$

Sensitivity: Sensitivity, also known as recall, measures the proportion of actual positives that are correctly identified.

$$Recall = \frac{TP}{TP+FN} \qquad (2)$$

Specificity: Specificity measures the proportion of actual negatives that are correctly identified.

$$Precision = \frac{TN}{TN+FP} \quad (3)$$

F1-Score: The F1-Score is the harmonic mean of precision and recall, providing a balance between the two. It is useful when the class distribution is imbalanced.

$$F1\ Score = \frac{2*(Precision\ *Recall\ )}{(Precision\ +Recall\ )} \quad (4)$$

Table Performance Measures of Binary Classification

Algorithm	Performance Measures (%)			
	Accuracy	Sensitivity	Specificity	F1-Score
CNN	98.08	97.14	100	98
ResNet	98.08	97.14	100	98

The table below shows a performance comparison between the CNN and ResNet models on the binary classification of lung cancer with respect to measures such as accuracy, sensitivity, specificity, and F1-Score. It is observed that both models performed similarly by exhibiting accuracy, sensitivity, specificity, and F1-Score values of 98.08%, 97.14%, 100%, and 98% respectively. From the findings above, it can be seen that both models performed extremely well in the classification of cancerous lungs from those that were not.

4.2 MULTICLASS CLASSIFICATION:-

For the problem of classification in multiple classes, the neural network had to classify each image of the CT scan into either of the three classes: normal lung, adenocarcinoma, and large cell carcinoma. Large cell carcinoma is one type of non-small cell lung carcinoma where it entails a presence of large abnormal cells, which are usually aggressive and grow at a fast pace. In their process of analyzing the data provided, the deep learning models were able to classify lung tissue images based on their characteristics.

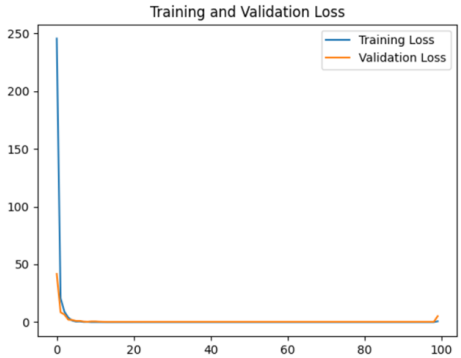

Here is the graph depicting the variation in losses for training and validation against the epoch in the case of the deep learning model. In the current graph, the horizontal axis represents the number of epochs, and the vertical axis represents the loss values. The training loss has been represented in blue color, and the validation loss has been represented in orange color. As can be seen in the graph, there is a very quick fall in losses at the initial stage, which means that the model learns well from the data.

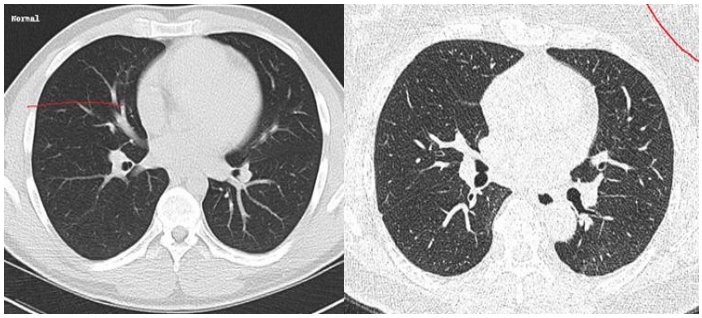

(a) (b)

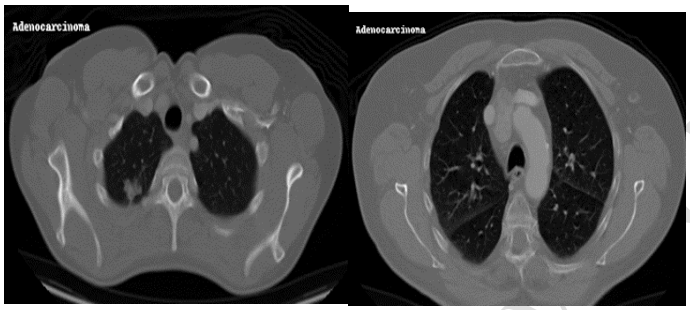

(c) (d)

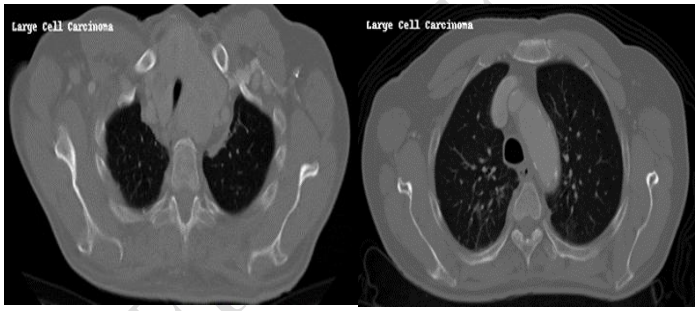

(e) (f)

Fig Result of Multiclass Classification with CNN (a) (b) Normal (c) (d) Adenocarcinoma (e) (f) Large cell carcinoma.The figure illustrates the results of a multi-class classification task utilizing CNN to differentiate between normal, adenocarcinoma, and large cell carcinoma based on medical imaging.

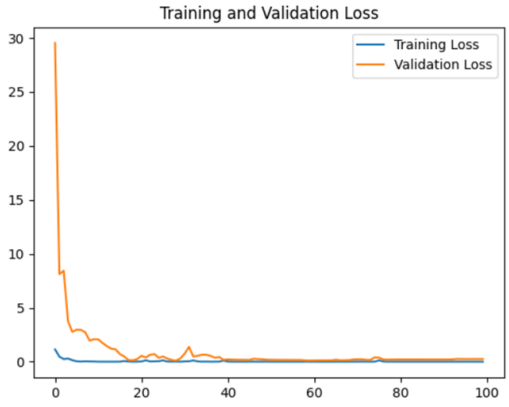

Figure 4.2.c presents the training history of the ResNet classifier. The blue curve indicates the training loss, while the orange curve is the validation loss. At first, the two losses are relatively high; however, with each epoch, they drop to lower values. The stable position of both lines implies effective learning and adequate

generalization ability of the model. The small rise in validation loss at the end could indicate the initial development of overfitting.

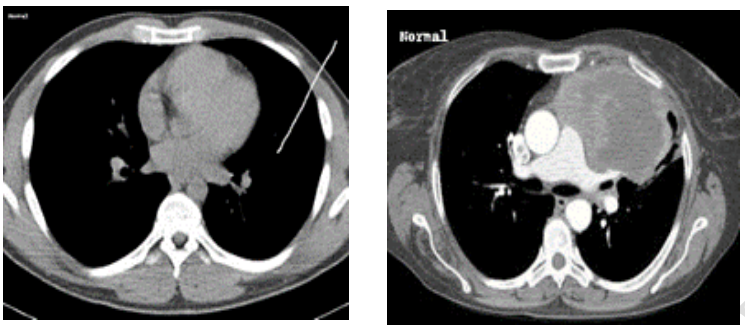

(a) (b)

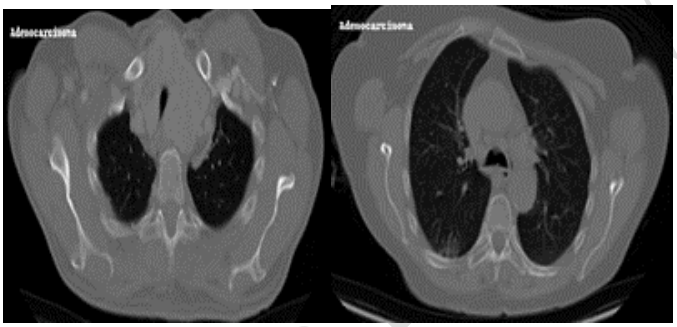

(c) (d)

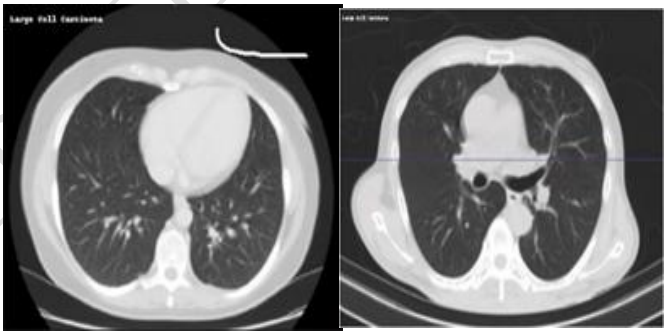

(e) (f)

Fig Results of Multi-class classification with Resnet (a) (b) Normal (c) (d)Adenocarcinoma (e) (f) Large cell carcinoma

Figure depicts the results of a multi-class classification task using ResNet to distinguish betweennormal, adenocarcinoma, and large cell carcinoma cases based on medical imaging.

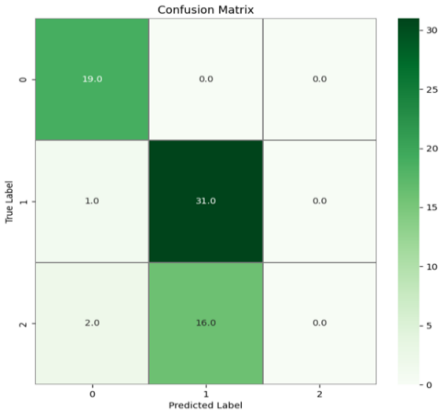

4.2.e. Confusion Matrix - Figure 4.2.e Confusion Matrix is a method of evaluating performance of an algorithm used for classification problems. Confusion Matrix is essentially an evaluation of the results of classification process. It consists of a table which compares the real target variables against the predicted target variables by machine learning algorithms. Vertical axis represents the real labels. In other words, it presents the real classes of the data. Horizontal axis represents the predicted labels. In other words, it presents the predictions of classes made by the model on the data. The numbers within confusion matrix represent the count of right or wrong predictions. Concerning above mentioned particular confusion matrix: Rows represent real labels of classes (0, 1, 2). Columns represent the predicted labels of classes (0, 1, 2). Values on diagonal (19, 31, 0) represent the count of correct predictions per class. This corresponds to True Positives (TP). There were 19 occurrences of class 0 that were predicted correctly. There were 31 occurrences of class 1 that were predicted correctly. There were 0 occurrences of class 2 that were predicted correctly.Classification Class 0: There is one mistake in classifying class 1 to class 0 and two in classifying class 2 to class 0.Classification Class 1: There are no cases of class 0 and sixteen of class 2 misclassified as class 1.Classification Class 2: There are no cases of class 0 and no cases of class 1 misclassified to class 2.The numbers on the non-diagonal cells in each row represent the cases of that row-class being misclassified as belonging to other classes. The off-diagonals represent False Negatives (FN). Class 0: There are no false negatives in class 0.Class 1: One case of class 1 is misclassified as class 0, while there are none in class 1 that is misrepresented as class 2.Class 2: Two cases of class 2 are misclassified as class 0, while 16 cases of class 2 are misrepresented as class 1.xIt works perfectly in prediction of class 1 where there were 31 cases predicted correctly but one wrong prediction. Also, it does not work well in predicting class 2 because of zero correct predictions but many wrong predictions to class 1. Confusion Matrix is an important tool in measuring the efficiency of classification and identifying errors in classification.

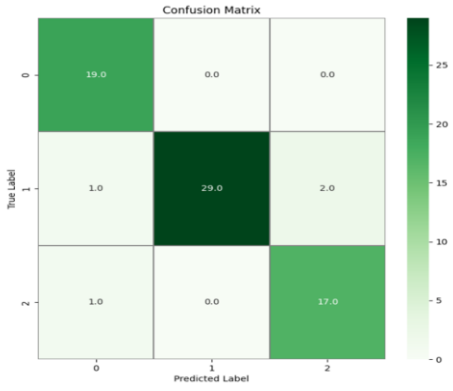

Fig Confusion Matrix of Multiclass Classification with ResNet

From the above confusion matrix for ResNet, it can be seen that for Class 0, 19 samples were predicted as Class 0, which corresponds to True Positive prediction. One sample was incorrectly predicted as Class 1, False negative prediction. In addition, one sample was predicted as Class 2, false negative prediction. For Class 1, 29 samples were predicted as Class 1, True Positive predictions. One sample was predicted as Class 0, False negative prediction, and two samples as Class 2, False Negative predictions. Finally, for Class 2, 17 samples were predicted as Class 2, True Positive predictions. Two samples were also predicted as Class 1, False

Negative predictions. Confusion matrix is an effective tool for assessing how good the classifier performs with respect to correct predictions and misclassification cases.

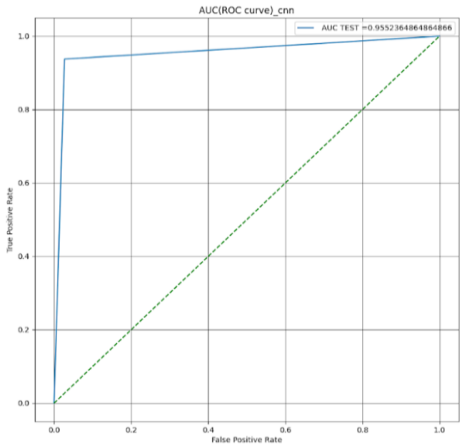

Fig 4.2.g. ROC curve of CNN

Figure below shows the Receiver Operating Characteristic (ROC) curve, which is a chart that visualizes the effectiveness of the binary classifier. The ROC curve consists of two axes; The X-axis is marked with "False Positive Rate," which is the percentage of true negatives that are wrongly classified as positive. Meanwhile, the Y-axis is marked with "True Positive Rate" and denotes the percentage of true positives that are correctly classified as positives. The Blue Line (ROC Curve) is the graphical representation of how the true and false positive rates vary at different threshold values. Ideally, the ROC will traverse vertically on the Y-axis up to the top left corner of the plot. The green dotted line (baseline) is the ROC curve of the random guess classifier.AUC (Area Under the Curve) is a criterion for evaluating the entire model, as it is an integrated value. AUC lies between 0 and 1, where 1 refers to the perfect model, and 0.5 is an indicator of a lack of discrimination capacity of the model. AUC is about 0.955 in the above picture; thus, one can conclude that the discrimination capacity of the model in question is rather high. Moreover, the above statement can be supported by the conclusion that the model in question has a high discrimination capacity. Additionally, the fact that the curve tends towards the upper-left part of the picture means that the true positive rate is quite high in terms of this model, while the false positive rate is quite low.

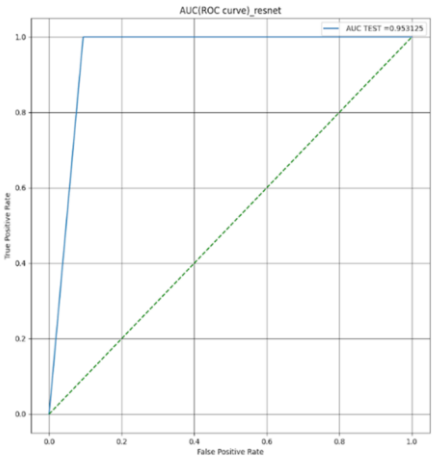

Fig ROC Curve of ResNet

Given below is the illustration of the Receiver Operating Characteristic (ROC) Curve, which is one of the methods of performance visualization of a binary classifier. True Positive Rate (TPR), also known as Sensitivity, is plotted on the y-axis, and it refers to the proportion of actual positives that are correctly classified as positives. On the other hand, False Positive Rate (FPR) is plotted on the x-axis, and it refers to the proportion of negatives that are falsely classified as positives. The blue curve in the figure represents the ROC curve. As the curve moves more toward the top left corner, the performance of the model increases. Diagonal Line is a ROC curve of a random classifier that does not have any discriminatory capacity.The value is used for

comparison purposes and acts as a standard. The Area Under the Curve (AUC) value of 0.953125 refers to the amount of space covered under the ROC curve. Area Under the Curve can have any value between zero and one; the higher its value is, the better will be the performance of the model. If the Area Under the Curve is equal to 0.5, there is no discrimination, but if it is equal to 1.0, then discrimination is perfect.

Table 4.2 Performance Measures of Multiclass Classification

Algorithm	Performance Measures (%)			
	Accuracy	Sensitivity	Specificity	F1-Score
CNN	96.65	100	94	92.68
ResNet	97.10	100	96	95

The table below summarizes the performance measures of CNN and RESNET for multi-class classification. The performance measures are expressed as percentages and include accuracy, sensitivity, specificity, and F1 score. The accuracy percentage value of CNN is 95.65%, whereas for RESNET, the value is 97.10%. The sensitivity measure refers to the percentage of positive cases actually detected by the model from all the actual positive cases. In both instances, the sensitivity of CNN and RESNET models is equal to 100%. The percentage value of specificity measures the percentage of actual negative values actually detected by the model. The specificity percentage value of CNN is 94% while that of RESNET is 96%. The F1 score is an additional metric provided by the two models, where the value of F1 score for CNN and RESNET are 92.68% and 95%, respectively.

PERFORMANCE COMPARISON WITH EXISTING ALGORITHM:-

Table 4.3 Performance measures with existing algorithm

Algorithm	Performance Measures (%)			
	Accuracy	Sensitivity	Specificity	F1 Score
KNN	93.6	88.4	100	94.5
SVM	97.4	100	94.3	97.5
Random Forest	97.4	95.3	100	97.8
AdaBoost	88.5	88.4	88.6	88.7
Inception V1	91.85	87.1	97.25	91.91
VGG16	93.56	89.92	97.71	93.70
AlexNET	95.73	95.20	96.33	95.97
Proposed Method	98.08	97.14	100	98.55

A comparison of the proposed model against the existing models with respect to the comparative performance shows that the proposed model outperforms existing models in terms of the accuracy rate due to the use of CNN and ResNet technology which give it a very high accuracy rate of 98.08%. As evident from the above graph, the proposed model outperforms existing models in terms of the accuracy rate. The distinguishing factor that makes this model superior to others in terms of efficiency is the use of CNN and ResNet. The CNN model enjoys

widespread recognition due to its capability of learning the hierarchical structure of the data automaticallyAs far as the ResNet technology is concerned, it should be admitted that this is only the improvement of the CNN technology. In this case, the feature extraction process with the use of CNN and deep learning techniques with the help of ResNet makes it much better than any other machine learning algorithm and other deep learning techniques. In such a way, it provides the opportunity for diagnosing the medical images with the high accuracy level and recognizing either benign or malignant conditions. In general, apart from improving the accuracy of the image analysis process to 98.08%, there are some other benefits.

CONCLUSION AND FUTURE SCOPE:-

The objective of this research was to diagnose lung cancer using Deep Learning algorithms on CT scans. Such preprocessing methods as resizing, filtering for noises, and augmentation of images have been used before feature extraction via Convolutional Neural Network algorithms. Binary and multiclass classification has been performed using both CNN and ResNet models. In terms of binary classification, the accuracy rate of each of the two models is 98.08%. For multiclass classification, the accuracy of the CNN model is 95.65%, whereas that of the ResNet model reaches 97.10%.

From the aforementioned findings, it is quite obvious that CNN and ResNet models, which have been suggested for the diagnosis of lung cancer, represent quite reliable tools. What is more important, the ResNet model surpasses the CNN model when it comes to performance at multiclass classification. Given such impressive results obtained during testing, the two models under discussion may be applied for practical use by radiologists and real-time analysis.

REFERENCES:-

[1] S. K. B. Sangeetha *et al.*, "An Enhanced Multimodal Fusion Deep Learning Neural Network for Lung Cancer Classification," *Systems and Soft Computing*, p. 200068, Dec. 2023, doi: 10.1016/j.sasc.2023.200068.

[2] S. Wankhade and V. S., "A novel hybrid deep learning method for early detection of lung cancer using neural networks," *Healthcare Analytics*, vol. 3, Nov. 2023, doi: 10.1016/j.health.2023.100195.

[3] I. Naseer, S. Akram, T. Masood, M. Rashid, and A. Jaffar, "Lung Cancer Classification Using Modified U-Net Based Lobe Segmentation and Nodule Detection," *IEEE Access*, vol. 11, pp. 60279–60291, 2023, doi: 10.1109/ACCESS.2023.3285821.

[4] A. A. Shah, H. A. M. Malik, A. H. Muhammad, A. Alourani, and Z. A. Butt, "Deep learning ensemble 2D CNN approach towards the detection of lung cancer," *Sci Rep*, vol. 13, no. 1, Dec. 2023, doi: 10.1038/s41598-023-29656-z.

[5] A. Davri *et al.*, "Deep Learning for Lung Cancer Diagnosis, Prognosis and Prediction Using Histological and Cytological Images: A Systematic Review," *Cancers*, vol. 15, no. 15. Multidisciplinary Digital Publishing Institute (MDPI), Aug. 01, 2023. doi: 10.3390/cancers15153981.

[6] D. Srivastava *et al.*, "Early Detection of Lung Nodules Using a Revolutionized Deep Learning Model," *Diagnostics*, vol. 13, no. 22, Nov. 2023, doi: 10.3390/diagnostics13223485.

[7] T. I. A. Mohamed, O. N. Oyelade, and A. E. Ezugwu, "Automatic detection and classification of lung cancer CT scans based on deep learning and ebola optimization search algorithm," *PLoS One*, vol. 18, no. 8 AUGUST, Aug. 2023, doi: 10.1371/journal.pone.0285796.

[8] N. Maleki and S. T. A. Niaki, "An intelligent algorithm for lung cancer diagnosis using extracted features from Computerized Tomography images," *Healthcare Analytics*, vol. 3, Nov. 2023, doi: 10.1016/j.health.2023.100150.

[9] A. Shimazaki *et al.*, "Deep learning-based algorithm for lung cancer detection on chest radiographs using the segmentation method," *Sci Rep*, vol. 12, no. 1, Dec. 2022, doi: 10.1038/s41598-021-04667-w.

[10] G. C. Forte *et al.*, "Deep Learning Algorithms for Diagnosis of Lung Cancer: A Systematic Review and Meta-Analysis," *Cancers*, vol. 14, no. 16. MDPI, Aug. 01, 2022. doi: 10.3390/cancers14163856.

[52] D. M. Ibrahim, N. M. Elshennawy, and A. M. Sarhan, "Deep-chest: Multi-classification deep learning model for diagnosing COVID-19, pneumonia, and lung cancer chest diseases," *Comput Biol Med*, vol. 132, May 2021, doi: 10.1016/j.compbiomed.2021.104348.

[53] T. L. Chaunzwa*et al.*, "Deep learning classification of lung cancer histology using CT images," *Sci Rep*, vol. 11, no. 1, Dec. 2021, doi: 10.1038/s41598-021-84630-x.

[54] L. Zhao *et al.*, "A Weighted Discriminative Extreme Learning Machine Design for Lung Cancer Detection by an Electronic Nose System," *IEEE Trans Instrum Meas*, vol. 70, 2021, doi: 10.1109/TIM.2021.3084312.

[55] Y. Xie *et al.*, "Early lung cancer diagnostic biomarker discovery by machine learning methods," *Transl Oncol*, vol. 14, no. 1, Jan. 2021, doi: 10.1016/j.tranon.2020.100907.

[56] G. Zhang *et al.*, "Philips (China) Investment Co., Ltd," 2021. [Online]. Available: www.ajcr.us/

[57] H. Yu, Z. Zhou, and Q. Wang, "Deep Learning Assisted Predict of Lung Cancer on Computed Tomography Images Using the Adaptive Hierarchical Heuristic Mathematical Model," *IEEE Access*, vol. 8, pp. 86400–86410, 2020, doi: 10.1109/ACCESS.2020.2992645.

[58] A. Masood *et al.*, "Automated Decision Support System for Lung Cancer Detection and Classification via Enhanced RFCN with Multilayer Fusion RPN," *IEEE Trans Industr Inform*, vol. 16, no. 12, pp. 7791–7801, Dec. 2020, doi: 10.1109/TII.2020.2972918.

[59] X. Wang *et al.*, "Weakly Supervised Deep Learning for Whole Slide Lung Cancer Image Analysis," *IEEE Trans Cybern*, vol. 50, no. 9, pp. 3950–3962, Sep. 2020, doi: 10.1109/TCYB.2019.2935141.

[60] P. M. Shakeel, M. A. Burhanuddin, and M. I. Desa, "Lung cancer detection from CT image using improved profuse clustering and deep learning instantaneously trained neural networks," *Measurement (Lond)*, vol. 145, pp. 702–712, Oct. 2019, doi: 10.1016/j.measurement.2019.05.027.

[61] Y. Xie *et al.*, "Knowledge-based Collaborative Deep Learning for Benign-Malignant Lung Nodule Classification on Chest CT," *IEEE Trans Med Imaging*, vol. 38, no. 4, pp. 991–1004, Apr. 2019, doi: 10.1109/TMI.2018.2876510.

[62] S. K. Lakshmanaprabu, S. N. Mohanty, K. Shankar, N. Arunkumar, and G. Ramirez, "Optimal deep learning model for classification of lung cancer on CT images," *Future Generation Computer Systems*, vol. 92, pp. 374–382, Mar. 2019, doi: 10.1016/j.future.2018.10.009.

[63] S. Pang, Y. Zhang, M. Ding, X. Wang, and X. Xie, "A Deep Model for Lung Cancer Type Identification by Densely Connected Convolutional Networks and Adaptive Boosting," *IEEE Access*, vol. 8, pp. 4799–4805, 2020, doi: 10.1109/ACCESS.2019.2962862.